Particle-assisted Formation of Oil-in-Liquid Metal Emulsions

Shreyas Kanetkar, Najam Ul H. Shah, Febby Krisnadi, Aastha Uppal, Rohit M. Gandhi, Michael D. Dickey, Robert Y. Wang, and Konrad Rykaczewski Robert Y. Wang, R

- 1. School for Engineering of Matter, Transport and Energy, Arizona State University, Tempe, AZ, 85287, USA
- 2. Department of Mechanical Engineering, University of Engineering and Technology, Taxila, 47050, Pakistan
- 3. Department of Chemical and Biomolecular Engineering, North Carolina State University, Raleigh, North Carolina 27695, USA
 - 4. Intel Corporation, 5000 W. Chandler Blvd., Chandler, AZ, 85226, United States

Keywords: liquid metal, foams, emulsions, silica, thermal interface materials, thermal conductivity, gallium-induced corrosion

Abstract

Gallium-based liquid metals (LM) have surface tension an order of magnitude higher than water and break up into micro-droplets when mixed with other liquids. In contrast, silicone oil readily mixes into LM foams to create oil-in-LM emulsions with oil inclusions. Previously, the LM was foamed through rapid mixing in air for an extended duration (over 2 hours). This process first results in the internalization of oxide flakes that form at the air-liquid interface. Once a critical fraction of these randomly shaped solid flakes is reached, air bubbles internalize into the LM to create foams that can internalize secondary liquids. Here, we introduce an alternative oil-in-LM emulsion fabrication method that relies on the prior addition of SiO₂ micro-particles into the LM before mixing it with the silicone oil. This particle-assisted emulsion formation process provides a higher control over the composition of the LM-particle mixture before oil addition, which we employ to systematically study the impact of particle characteristics and content on the emulsions' composition and properties. We demonstrate that the solid particle size (0.8 µm to 5 µm) and volume fraction (1% to 10%) have a negligible impact on the internalization of the oil inclusions. The inclusions are mostly spherical with diameters of 20 to 100 µm diameter and are internalized by forming new, rather than filling old, geometrical features. We also study the impact of the particle characteristics on the two key properties related to the functional application of the LM emulsions in the thermal management of microelectronics. In particular, we measure the impact of particles and silicone oil on the emulsion's thermal conductivity and its ability to prevent deleterious gallium-induced corrosion and embrittlement of contacting metal substrates.

Keywords: liquid metals, materials with liquid inclusions, emulsions, foams

^{*}Corresponding author emails: rywang@asu.edu, konradr@asu.edu

1. Introduction

Gallium and its alloys have metallic properties while being liquid near room temperature and are used to make stretchable and soft components and devices for electronics, biomedical, sensors, catalysis, energy storage, and thermal management applications [1–7]. Adding solid particles to these liquid metals (LM) can positively augment their transport, rheological, and adhesive properties [2,3,8,9]. Accordingly, LM has been mixed with many solids particles including Cu [10–13], Fe [13–15], Ni [16–20], Ag [20–22], Mg [23], Gd [24], BN [23], W [25], SiC [26], SiO₂ [27,28], Cu-Fe [29], steel [15], diamond [30], graphene [31], and carbon nanotubes [32,33]. As alternatives to solid particles, air bubbles can also be internalized in LM to make foams.

Pure LMs can be foamed by the rapid mixing of the liquid in air for an extended duration (*e.g.*, 600 rpm for 120 minutes [34,35]). Before foaming occurs (*i.e.*, incorporation of air bubbles into the LM), a critical volume fraction of microscopic oxide flakes that form at the air-liquid interface must be internalized into the bulk of the LM [34,35]. We recently demonstrated that LM also foams when the liquid is manually mixed for a short period with even a small volume fraction of SiO₂ micro-particles [36]. One of the most interesting characteristics of the LM foams is that they enable the internalization of insoluble liquid inclusions into the LM [37–40].

LM breaks up into droplets when mixed with other insoluble liquids such as silicone oil [41]. In contrast, LM foams made through stirring and oxide-flake incorporation readily internalize up to 40% volume fraction of oil inclusion to make silicone oil-in-LM emulsions (we refer to this process as "oxide-assisted" oil-in-LM emulsion formation) [37,38]. Similar emulsions have also been created, albeit with smaller control over the content of the secondary liquid, by increasing the volume fraction of GaInSn within polydimethylsiloxane until phase inversion occurred [42]. Oxide flakes are also likely generated during the processes, but their characteristics and content are

difficult to quantify. Likewise, it is difficult to quantify the volume fraction and size distribution of the oxide flakes that spontaneously form and mix into LM during mechanical stirring. Therefore, the role that solid particles play in enabling the addition of the secondary liquid inclusions into LM is unclear.

Here, we introduce an alternative method to incorporate secondary liquid inclusions into LM that provides higher control over the mixture's composition. Specifically, we demonstrate that silicone oil inclusions are also readily incorporated into LM briefly manually mixed (20 minutes at 120 rpm) with SiO₂ micro-particles (see fabrication schematic in Figure 1 (a) and example cross section of the emulsion illustrating various features including air bubbles and silicone oil inclusions in Figure 1 (b)). This process reduces oxide flake formation and incorporation into LM associated with foaming via extended mechanical stirring (120 minutes at 600 rpm). We employ this new particle-assisted silicone oil-in-LM emulsion fabrication method to more systematically explore the relation between added solid particle size and fraction and the incorporation of the oil inclusions. We also study the impact of the particle characteristics on the two key properties related to the functional application of the LM emulsions in the thermal management of microelectronics. In particular, we measure the impact of particles and silicone oil on the emulsion's thermal conductivity and its ability to prevent deleterious gallium-induced corrosion and embrittlement of contacting metal substrates [37,38].

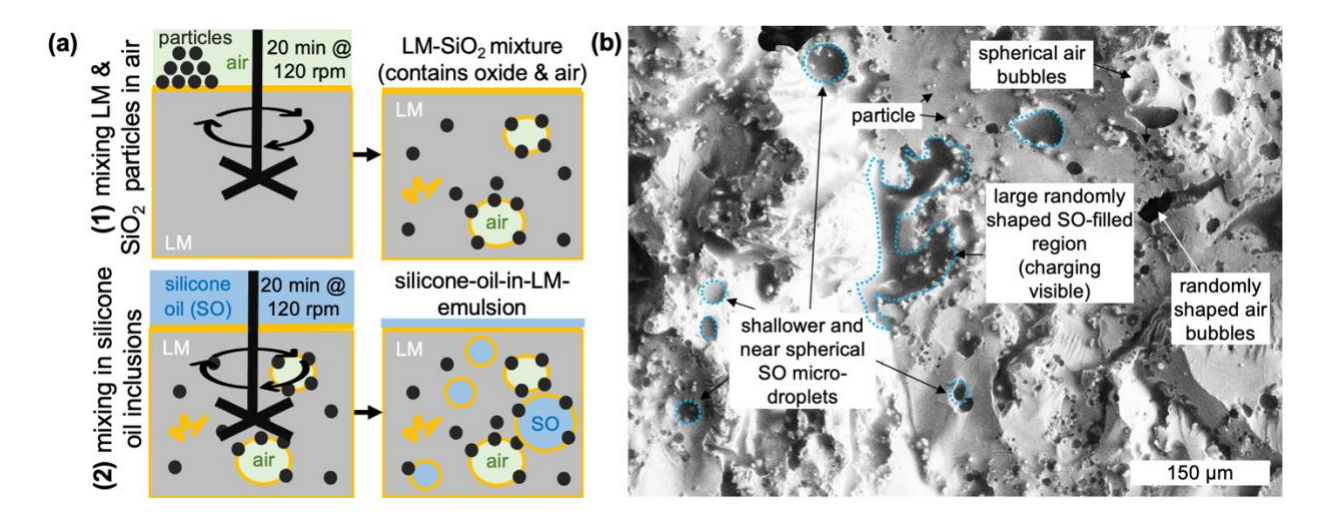


Figure 1. (a) Schematic showing the fabrication of LM-SiO₂ mixture and subsequent silicone oil-in-LM emulsions (i.e., after silicone oil addition) and **(b)** representative cross-sectional electron micrograph for such an emulsion made using a LM-SiO₂ mixture with 5% volume fraction of 5 μm SiO₂ particles (defined prior to oil addition) and 20% mixing volume fraction of silicone oil.

2. Methods

We purchased gallium (Ga, 99.99% purity) metal from Rotometals, the SiO₂ particles from US Research Nanomaterials (mostly spherical in shape with diameters of 0.8 μm and 5 μm; particle size distribution is available in Kanetkar *et al.*[36]), and silicone oil with 10 cSt viscosity from Sigma-Aldrich. We combined these materials into the emulsions in a two-step process. First, we manually mixed 20 g of liquid gallium with the SiO₂ particles with 1%, 2.5%, 5%, and 10% particle volume fraction in gallium. The particle volume fractions are defined and reported with respect to the original mass of LM (i.e., prior to silicone oil addition). Subsequently, we manually mixed 5 g of the LM-SiO₂ mixtures with the desired amount of 10 cSt silicone oil. We mixed the samples in a plastic weigh boat for 30 minutes at ~120 rpm using a wooden rod of diameter 1.2 mm. We note that at the end of mixing a minute quantity of oil will be left over on the weigh boat and the surface of the wooden rod. We weighed the wooden rod and weigh boats before and after mixing to

measure the incorporated silicone oil volume. We refer to the mixing volume fraction of the oil because a small portion of it inevitably remains on, for example, the walls of the mixing vessel, so the actual internalized volume fraction is slightly smaller (see Figure S2 in the Supplemental Material—SM). We conducted the density and thermal conductivity measurements as well as cryogenic imaging using the same procedures as in our prior work [37,38,43,44] and refer the reader to those works for further details.

3. Results

3.1. Impact of particle size and volume fraction on silicone oil inclusion internalization

Since we recently found that particle size and volume fraction impact air internalization into LM [36], we explored the impact of these parameters on the silicone oil-in-LM emulsion formation process. To do so, we mixed varied volume fractions of silicone oil with LM-SiO₂ mixtures containing 1 to 10% volume fraction of particles with average diameters of 0.8 µm or 5 µm. We selected to make LM-SiO₂ mixtures with these two particle sizes because adding particles smaller than 0.8 µm makes the LM and particle mixture highly viscous and challenging to mix [36,45], while mixing in the 5 µm particles leads to LM mixtures with nearly the same properties as those with larger particles [36]. Irrelevant of particle size, we were able to mix a 20%, 30%, and 40% volume fraction of the silicone oil into the LM-SiO₂ mixtures with 1%, 2.5%, and 5% volume fraction of the particles. Increasing the particle content from 5% to 10% did not increase the silicone oil capacity (i.e., as in the emulsions made using the oxide-assisted method [37,38], 40% volume fraction of silicone oil is the saturation limit). As a control experiment, we checked that LM mixed for 20 minutes without the particles breaks up into droplets when mixed even with just a 20% volume fraction of silicone oil.

The plot in Figure 2 (a) shows the density of LM-SiO₂ with varied particle sizes and volume fractions before and after the addition of 20% volume fraction of silicone oil that all LM paste compositions can absorb. The LM-SiO₂ pastes made with the 0.8 µm particles internalize more air than those with 5 µm particles [36], and therefore, emulsions made with the 0.8 µm particles are less dense. Similarly, the LM foam density decreases with the particle volume fraction, leading to decrease of the emulsion density with particle content. We note that the LM-SiO₂ mixtures and the resulting emulsions containing 1 and 2.5% volume fraction of the particles had a buoyant layer underneath the top surface containing particles, gallium oxide, air bubbles, and oil droplets. While also present in the LM-SiO₂ mixtures with 5% volume fraction of the particles, the buoyant layer occupyies most of the sample. In turn, the LM-SiO₂ mixtures with 10% volume fraction of the particles did not have any unmixed liquid metal, but was highly viscous and difficult to manually mix with the silicone oil. Accordingly, to gain insight into the mechanism of silicone oil internalization, we measured the density variation of emulsions made with 5% particle volume fraction as function of the silicone oil content.

Silicone oil can be incorporated into the LM pastes or foams by replacing air in existing geometrical features (*e.g.*, surface pores) or adding new micro-droplets into the bulk of the liquid, which we refer to as the "replacement" mechanism and "addition" mechanism, respectively [38]. We note that such oil inclusions grow an oxide shell nearly instantaneously, becoming silicone oil capsules [38]. We previously demonstrated that the replacement and addition mechanisms of oil incorporation during oxide-assisted emulsion formation can be distinguished from one another via the relationship between the incorporated oil volume fraction and the resulting emulsion density [38]. In particular, the density of emulsion formed through the addition mechanism decreases as a function of the silicone oil [38]. The plot in **Figure 2** (b) shows that the density decreases linearly

at the same rate with the silicone oil mixing-in volume fraction for both of the particles sizes, indicating that the internalization occurs through formation of new silicone oil droplets and is independent of the particle size (see further details in the SM). Next, we use electron microscopy to investigate whether the particle characteristics impact the microscale features of the silicone oil inclusions in the emulsions.

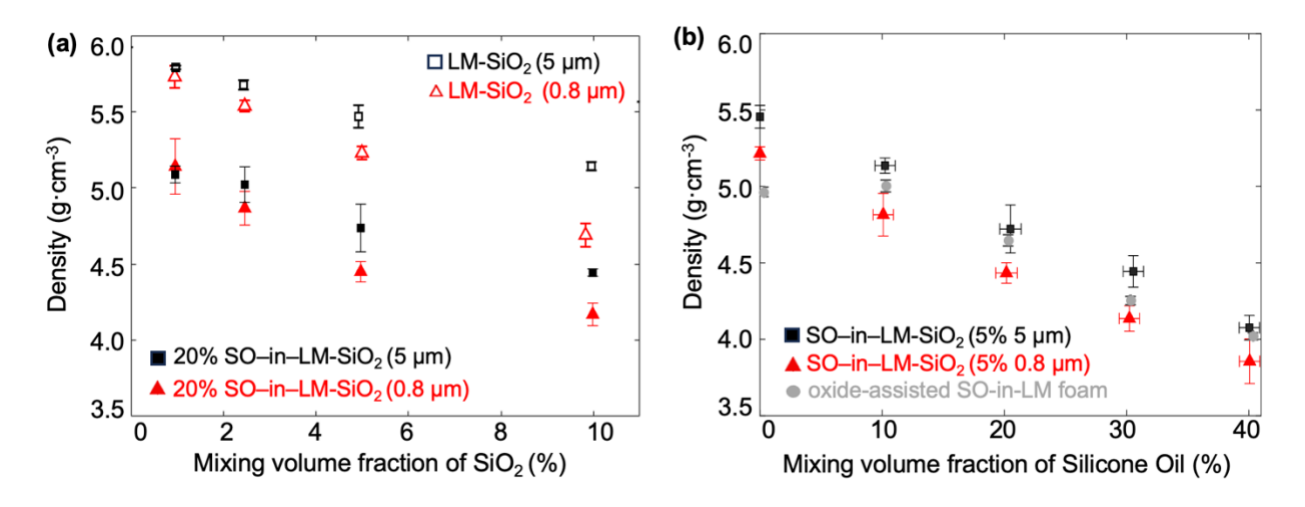


Figure 2. Plot of the density of LM-SiO₂ mixture and corresponding emulsions (i.e., after silicone oil addition) with **(a)** 20% mixing volume fraction of silicone oil as a function of the SiO₂ particle volume fraction (defined prior to oil addition) and **(b)** with 5% volume fraction of SiO₂ particle as a function of the mixing in volume fraction of the silicone oil. Reference data for oxide-assisted SO-in-LM foam emulsions are also shown [38].

We froze, cross-sectioned, and imaged the samples using cryogenic scanning electron microscopy (cryo-SEM) to reveal the internal structure of the emulsions made with varied oil content. The electron micrographs in **Figures 3(a)** and **3(b)** show that all samples contain nearly spherical silicone oil inclusions with diameters ranging from 20 to 100 μm. The particles aggregate on air bubble and LM interfaces in the LM-SiO₂ mixtures prior to silicone oil addition [36], but

do not preferentially accumulate on the walls of the silicone oil inclusions. We also did not observe preferential aggregation of the particles into the silicone oil. However, as the oil volume fraction increased, we occasionally observed irregularly shaped oil inclusions with large particle clusters. Unfortunately, cross-sectioning of the emulsions with 30% and 40% mixing volume fraction of the silicone oil led to bleeding-out of the oil over parts of the exposed cross-section surface and associated difficulty in imaging the sample structures (see charging in the zoomed-out micrographs). Next, we measure the impact of the particle characteristics on the thermal conductivity of the emulsions.

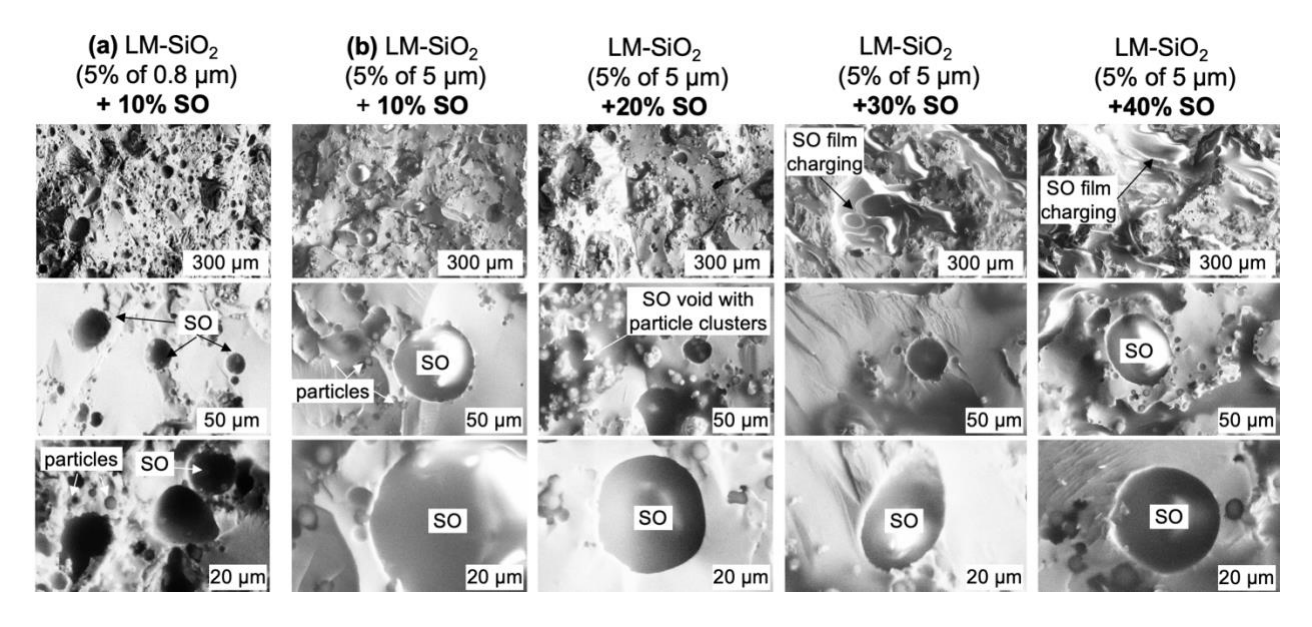


Figure 3. Cross-sectional cryogenic electron micrographs of **(a)** LM-SiO₂ mixture containing 5% of 0.8 μm particles with 10% of silicone mixing volume fraction of silicone oil and of **(b)** LM-SiO₂ mixture containing 5% of 5 μm SiO₂ particles with 10% to 40% volume fraction of silicone oil added.

3.2. Impact of particle characteristics on the thermal conductivity of the silicone oil-in-LM emulsions

Figure 4 (a) shows the thermal conductivity values measured for emulsions made using the particle-assisted method and our prior measurements for those made using the oxide-assisted method [37,38]. Adding 5% of 0.8 μm or 5 μm SiO₂ particles to the LM results in a much smaller thermal conductivity decrease (from about 35.4 W·m⁻¹K⁻¹ for pure gallium to about 28 W·m⁻¹K⁻¹ for 5 µm particles and to about 25 W·m⁻¹K⁻¹ for 0.8 µm particles) than foaming the liquid in air through stirring for 2 hours (about 19 W·m⁻¹K⁻¹). However, once silicone oil is added to the LM-SiO₂ mixture or LM foams, all emulsions' thermal conductivity, regardless of fabrication method or particle size, is comparable for a given silicone oil volume fraction. Figure 4 (b) shows that the thermal conductivity is insensitive to the SiO₂ particle volume fraction within the 1 to 10% volume fraction range (since particle size did not impact the thermal conductivity, we only tested the impact of volume fraction of 0.8 µm particles). Increasing the volume fraction of silicone oil decreases the thermal conductivity, reducing it to the 13 to 17 W·m⁻¹K⁻¹ range for 10% silicone oil mixing volume fraction and the 7 to 10 W·m⁻¹K⁻¹ range for 40% silicone oil mixing volume fraction. We note that minor scatter in the thermal conductivity of emulsions made using various approaches (most prominent at 30% mixing silicone oil fraction) likely stems from a shift introduced by presenting the plot in terms of mixing volume fraction of the silicone oil. In particular, the scatter in the thermal conductivity is reduced when it is presented in terms of actual volume fraction of incorporated silicone oil (which varies in ways that are dependent on the fabrication method) or in terms of the emulsion density (see the SM). Thus, the fabrication method, particle size, and volume fraction have very minor impacts on the thermal conductivity of the

emulsions. Next, we explore if these parameters impact the corrosive characteristics of the emulsions.

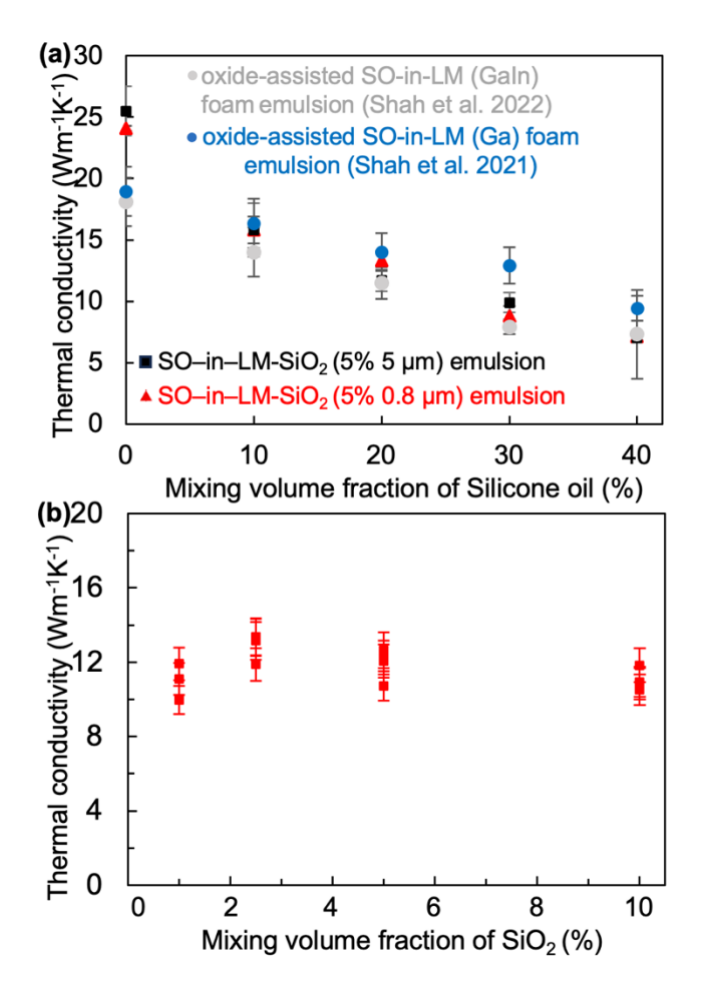


Figure 4. (a) The effective thermal conductivity of the silicone oil (SO)-in-LM emulsions made using oxide-assisted method with Ga foam from Shah et al. 2021 [37] and with GaIn foam from Shah et al. 2022 [38] and particle-assisted (5% SiO₂ particles) method as a function of mixing volume fraction of silicone oil and **(b)** thermal conductivity of an emulsion made by mixing 20% SO with LM- SiO₂ made with varied volume fractions of 0.8 μm SiO₂ particles.

3.3 Prevention of gallium-induced corrosion on contacting aluminum surface

Gallium and its alloys can corrode or embrittle most other metals they come in contact with [46], so their implementation in microelectronics packaging requires additional components such as barrier films or gaskets. Our previous work revealed that the exterior silicone oil film on the emulsions with a 40% volume fraction of silicone oil made using the oxide-assisted method prevented gallium-induced embrittlement of contacting aluminum substrates [37,38]. To confirm that emulsions made using the particle-assisted method also have an exterior silicone oil film, we measured their wetting properties. **Figure 5 (a)** shows that the contact angles of water droplets on the surface of the particle-assisted emulsions with 5 μm particles are 75° to 85° (i.e., the surface is slightly hydrophilic) while those with 0.8 μm particles are 90° to 100° (i.e., the surface is hydrophobic). In addition, as on typical of lubricant-impregnated surfaces [44], an oil meniscus is clearly visible on the edge of all the droplets. Emulsions made using the oxide-assisted method displayed similar contact angles [37], while those of LM-SiO₂ and LM foams without oil are highly hydrophilic. Next, we describe how the external oil film contributes to the corrosion barrier characteristics of the emulsions.

Using our prior approach of compressing a film of the emulsion between two aluminum foil sheets for 24 hours (see **Figure 5 (b)**), we quantified the percentage of samples visibly corroded by the emulsions made using the particle-assisted method. As expected, the control LM foam and LM-SiO₂ mixtures without oil corroded all contacting aluminum (*i.e.*, 0% corrosion protection). We achieved poor results with emulsions made from LM-SiO₂ mixtures with the 30% volume fraction of silicone oil (*e.g.*, 0% protection for 5% of the 5 μm SiO₂ particles in preliminary testing). The bar plot in **Figure 5 (c)** shows that the corrosion prevention of the emulsions made using the particle-assisted method highly depends on the particles' size. In particular, the emulsions made with the 5% volume fraction of the 5 μm particles and the 40% volume fraction of silicone

oil only protected about 25% of samples against corrosion. In contrast, for the same volume percent of silicone oil, we found that the emulsions made with the 0.8 μm particles demonstrated the best prevention against corrosion with ~97% protection level (*i.e.*, 31 out of 32 contacting aluminum foil samples did not corrode). We note that the exterior silicone oil layer provides a thin electrically insulating skin on the emulsions. However, electrical probes easily pierce this skin, and casual measurements demonstrate that the emulsion interior is electrically conductive.

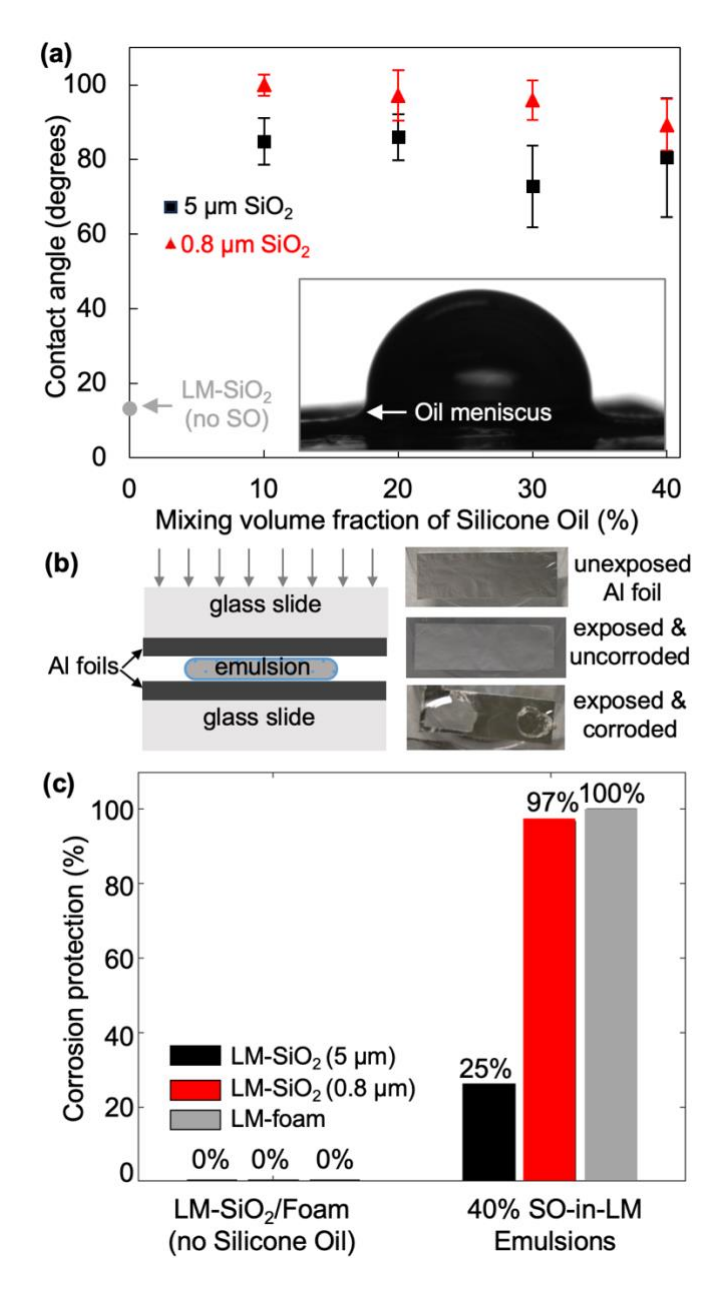


Figure 5. (a) The water contact angles of LM mixtures containing 5% of SiO₂ particles and corresponding emulsions; inset shows a representative image of a water droplet on a silicone oil-in-LM emulsion fabricated using particle-assisted method; **(b)** schematic of the corrosion testing experimental setup and example results of Al foil prior to and after exposure to LM emulsion (*i.e.*, uncorroded or corroded), and **(c)** bar plot of the percentage of aluminum samples that did not corrode upon contact with the specified LM foam/paste or silicone oil (SO)-in-LM emulsions.

4. Discussion

We demonstrated that mixing silicone oil with a priori made LM and SiO₂ micro-particle mixtures can make silicone oil-in-LM emulsions. The silicone oil inclusions are mostly spherical and have diameters in the 20 to 100 µm range. Their spherical shape implies that they were incorporated into LM by creating new geometrical features (i.e., the oil droplets) rather than filling in existing air bubbles or pores that tend to be irregularly shaped. This inclusion internalization mechanism is also confirmed by the linear decrease of the emulsion density with the silicone oil volume fraction [38]. Our results also show that particle size between 0.8 μm and 5 μm and volume fraction between 1% to 10% have negligible impact on silicone oil internalization or the thermal conductivity of the emulsions. The density and thermal conductivity of the emulsions made using the particle-assisted method are also about the same as those made using the oxide-assisted method, implying that the fabrication method has a minor impact on the resulting material. A sideby-side comparison of emulsions made using the two methods with the same silicone oil content in the SM demonstrates only some internal structure differences. The particle size only greatly impacted the emulsion's ability to prevent gallium-induced embrittlement of contacting aluminum foils. To understand the underlying mechanism, we next inspect the silicone oil layers on the exterior surfaces of the emulsions.

The cryogenic electron micrographs in **Figure 6 (a)-(c)** show that the exterior surface of the LM-SiO₂ mixtures is smoother than that of the LM foams. Once the oil is added, the smoother surfaces support a "patchier" layer of silicone oil compared to the rougher and porous surface of the LM foam that supports a continuous silicone oil film. To provide a more quantitative insight, we used a focused ion beam (FIB) to reveal the near-surface cross-section of the emulsion. As

shown in Figure 6 (d), the process of FIB cross-sectioning requires the deposition of a protective organometallic layer (mainly platinum in an amorphous carbon matrix). Confirming our surface observations, the micrographs of the FIB-cut cross-sections show that the silicone oil thickness varies from up to approximately 0.5 µm, which we also observed for the emulsions made with the oxide-assisted method [38], to nearly unobservable values (the slight vibration associated with the cooling nitrogen gas flow in the cryogenic SEM stage worsen the typical sub-10 nm resolution). Consequently, the rare failure (1 in 32 samples) to prevent gallium corrosion of the contacting aluminum surface likely comes from breaching of such locally extremely thin silicone layers on the emulsions with 0.8 µm particles. In contrast, the more porous surface of the LM foams shown in Figure 6 (c) supports a thick and continuous silicone oil film that, at least in our measurements, is not breached by compression with an aluminum surface. Although hard to quantify due to the mentioned limitations of the cryogenic surface and cross-sectional imaging, the emulsions with the 5 µm particles likely have a patchier silicone film that is easier to breach (or have partially exposed LM surface), therefore inducing more corrosion of contacting aluminum foil. The 10 to 20° lower water droplet contact angles on these emulsions also support the notion of partially exposed hydrophilic LM surface (covered by hydrophilic oxide). Having this understanding might open avenues for simple modification of the surface of the emulsions made with the particleassisted method to induce complete corrosion prevention (e.g., roughening the surface through shaking of the sample for an extended period that leads to excessive oxide formation and wrinkling).

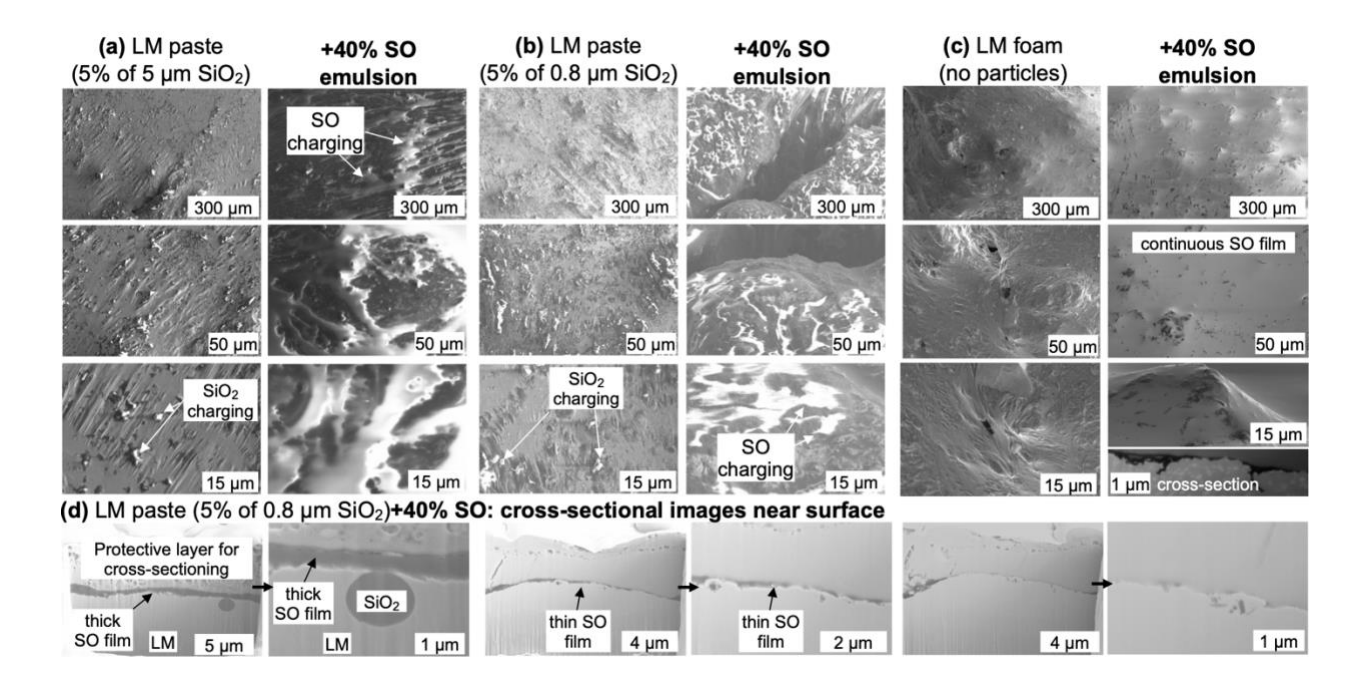


Figure 6. Cryogenic electron micrographs of **(a)-(c)** the exterior surface of **(a)** the LM-SiO₂ mixture containing 5% of 5 μm SiO₂ particles and corresponding 40% silicone oil (SO) emulsion, **(b)** the LM-SiO₂ mixture containing 5% of 0.8 μm SiO₂ particles and corresponding 40% SO emulsion, and **(c)** LM foam (oxide-assisted fabrication without particles) and corresponding 40% SO emulsion, and **(d)** cross-sectional images of cryogenic FIB cuts at the surface of the emulsion shown in **(b)**.

5. Conclusions

We demonstrated that silicone oil-in-LM emulsions can be fabricated by mixing the oil with LM-SiO₂ mixtures containing 1 to 10 % of SiO₂ micro-particles. As those made using the oxide-assisted method, the emulsions made using the particle-assisted method with 0.8 μm and 5 μm SiO₂ particles can internalize up to about 40% volume fraction of silicone oil. The 20 to 100 μm diameter silicone oil inclusions within the LM are primarily spherical and are internalized by forming new, rather than filling old, geometrical features. The SiO₂ particle size and volumetric

content have a negligible impact on the silicone oil internalization and thermal conductivity of the emulsions. These properties are comparable to those of the emulsions made using the prior oxide-assisted method. However, using water contact angle measurements and cryogenic near-surface imaging, we revealed that there also is a highly non-uniform silicone oil surface layer on the emulsions made using the particle-assisted method. Lower water droplet contact angles imply that the exterior oil non-uniformity is greater on the emulsions made with 5 µm SiO₂ particles, which translated into drastically different corrosion prevention characteristics. In particular, emulsions with 40% silicone oil fraction made with LM pastes with 5 µm SiO₂ particles corrode most of the contacting aluminum samples. In contrast, those made with 0.8 µm SiO₂ particles prevent such failure in nearly all cases (31/32 tests). In contrast to the original oxide-assisted fabrication method, the introduced particle-assisted oil-in-LM emulsion fabrication method opens up extensive opportunities for the compositional engineering of LM composites containing both liquid inclusions and solid additives.

Acknowledgments

We acknowledge the use of facilities within the Eyring Materials Center at Arizona State University supported in part by NNCI-ECCS-2025490. This research was funded by National Science Foundation Division of Civil, Mechanical and Manufacturing Innovation grant 2032415.

References

[1] Daeneke T, Khoshmanesh K, Mahmood N, de Castro I A, Esrafilzadeh D, Barrow S J, Dickey M D and Kalantar-Zadeh K 2018 Liquid metals: fundamentals and applications in chemistry *Chem Soc Rev* **47** 4073–111

- [2] Chen S, Wang H-Z, Zhao R-Q, Rao W and Liu J 2020 Liquid metal composites *Matter* **2** 1446–80
- [3] Malakooti M H, Bockstaller M R, Matyjaszewski K and Majidi C 2020 Liquid metal nanocomposites *Nanoscale Adv* **2** 2668–77
- [4] Chen S, Deng Z and Liu J 2020 High performance liquid metal thermal interface materials *Nanotechnology* **32** 092001
- [5] Lu Y, Hu Q, Lin Y, Pacardo D B, Wang C, Sun W, Ligler F S, Dickey M D and Gu Z 2015 Transformable liquid-metal nanomedicine *Nat Commun* **6**
- [6] Handschuh-Wang S, Stadler F J and Zhou X 2021 Critical review on the physical properties of gallium-based liquid metals and selected pathways for their alteration *The Journal of Physical Chemistry C* **125** 20113–42
- [7] Liu S, Sun X, Hildreth O J and Rykaczewski K 2015 Design and characterization of a single channel two-liquid capacitor and its application to hyperelastic strain sensing *Lab Chip* **15**
- [8] Dickey M D 2014 Emerging applications of liquid metals featuring surface oxides ACS Appl Mater Interfaces **6** 18369–79
- [9] Neumann T v., Facchine E G, Leonardo B, Khan S and Dickey M D 2020 Direct write printing of a self-encapsulating liquid metal-silicone composite *Soft Matter* **16** 6608–18
- [10] Li G, Ji Y, Wu M and Ma H 2016 Highly Conductive thermal paste of liquid matal alloy dispersed with copper particles *Proceedings of the ASME 2016 heat transfer summer conference* (Wahington DC)
- [11] Tang J, Zhao X, Li J, Guo R, Zhou Y and Liu J 2017 Gallium-Based Liquid Metal Amalgams: Transitional-State Metallic Mixtures (TransM2ixes) with Enhanced and Tunable Electrical, Thermal, and Mechanical Properties *ACS Appl Mater Interfaces* **9** 35977–87
- [12] Ralphs M I, Kemme N, Vartak P B, Joseph E, Tipnis S, Turnage S, Solanki K N, Wang R Y and Rykaczewski K 2018 In Situ Alloying of Thermally Conductive Polymer Composites by Combining Liquid and Solid Metal Microadditives *ACS Appl Mater Interfaces* **10** 2083–2092
- [13] Tutika R, Zhou S H, Napolitano R E and Bartlett M D 2018 Mechanical and Functional Tradeoffs in Multiphase Liquid Metal, Solid Particle Soft Composites *Adv Funct Mater* **28** 1804336
- [14] Ren L, Sun S, Casillas-Garcia G, Nancarrow M, Peleckis G, Turdy M, Du K, Xu X, Li W, Jiang L, Dou S X and Du Y 2018 A Liquid-Metal-Based Magnetoactive Slurry for Stimuli-Responsive Mechanically Adaptive Electrodes *Advanced Materials* **30** 1802595
- [15] Carle F, Bai K, Casara J, Vanderlick K and Brown E 2017 Development of magnetic liquid metal suspensions for magnetohydrodynamics *Phys Rev Fluids* **2** 013301
- [16] Guo R, Wang X, Chang H, Yu W, Liang S, Rao W and Liu J 2018 Ni-Galn Amalgams Enabled Rapid and Customizable Fabrication of Wearable and Wireless Healthcare Electronics *Adv Eng Mater* **20** 1800054
- [17] Wang X, Guo R, Yuan B, Yao Y, Wang F and Liu J 2018 Ni-doped Liquid Metal Printed Highly Stretchable and Conformable Strain Sensor for Multifunctional Human-Motion Monitoring 2018 40th Annual International Conference of the IEEE Engineering in Medicine and Biology Society (EMBC) (IEEE) pp 3276–9

- [18] Ralphs M, Kong W, Wang R Y and Rykaczewski K 2019 Thermal Conductivity
 Enhancement of Soft Polymer Composites through Magnetically Induced Percolation and
 Particle—Particle Contact Engineering Adv Mater Interfaces 6 1801857
- [19] Daalkhaijav U, Yirmibesoglu O D, Walker S and Mengüç Y 2018 Rheological Modification of Liquid Metal for Additive Manufacturing of Stretchable Electronics Adv Mater Technol 3 1700351
- [20] Tang J, Zhao X, Li J, Zhou Y and Liu J 2017 Liquid Metal Phagocytosis: Intermetallic Wetting Induced Particle Internalization *Advanced Science* **4** 1700024
- [21] Lin Z, Liu H, Li Q, Liu H, Chu S, Yang Y and Chu G 2018 High thermal conductivity liquid metal pad for heat dissipation in electronic devices *Appl Phys A Mater Sci Process* **124** 368
- [22] Tavakoli M, Malakooti M H, Paisana H, Ohm Y, Green Marques D, Alhais Lopes P, Piedade A P, de Almeida A T and Majidi C 2018 EGaln-Assisted Room-Temperature Sintering of Silver Nanoparticles for Stretchable, Inkjet-Printed, Thin-Film Electronics *Advanced Materials* **30** 1801852
- [23] Wang X, Yao W, Guo R, Yang X, Tang J, Zhang J, Gao W, Timchenko V and Liu J 2018 Soft and Moldable Mg-Doped Liquid Metal for Conformable Skin Tumor Photothermal Therapy *Adv Healthc Mater* **7** 1800318
- [24] De Castro I A, Chrimes A F, Zavabeti A, Berean K J, Carey B J, Zhuang J, Du Y, Dou S X, Suzuki K, Shanks R A, Nixon-Luke R, Bryant G, Khoshmanesh K, Kalantar-Zadeh K and Daeneke T 2017 A Gallium-Based Magnetocaloric Liquid Metal Ferrofluid *Nano Lett* 17 7831–8
- [25] Kong W, Wang Z, Wang M, Manning K C, Uppal A, Green M D, Wang R Y and Rykaczewski K 2019 Oxide-Mediated Formation of Chemically Stable Tungsten–Liquid Metal Mixtures for Enhanced Thermal Interfaces *Advanced Materials* **31**
- [26] Kong W, Wang Z, Casey N, Korah M M, Uppal A, Green M D, Rykaczewski K and Wang R Y 2021 High Thermal Conductivity in Multiphase Liquid Metal and Silicon Carbide Soft Composites Adv Mater Interfaces 2100069
- [27] Chang H, Zhang P, Guo R, Cui Y, Hou Y, Sun Z and Rao W 2020 Recoverable liquid metal paste with reversible rheological characteristic for electronics printing *ACS Appl Mater Interfaces* **12** 14125–35
- [28] Yuan B, Zhao C, Sun X and Liu J 2020 Lightweight Liquid Metal Entity *Adv Funct Mater* 1910709
- [29] Li F, Kuang S, Li X, Shu J, Li W, Tang S and Zhang S 2019 Magnetically-and Electrically-Controllable Functional Liquid Metal Droplets *Adv Mater Technol* **4** 1800694
- [30] Wei S, Yu Z, Zhou L and Guo J 2019 Investigation on enhancing the thermal conductance of gallium-based thermal interface materials using chromium-coated diamond particles *Journal of Materials Science: Materials in Electronics* **30** 7194–202
- [31] Sargolzaeiaval Y, Ramesh V P, Neumann T V., Miles R, Dickey M D and Öztürk M C 2019 High Thermal Conductivity Silicone Elastomer Doped with Graphene Nanoplatelets and Eutectic Galn Liquid Metal Alloy *ECS Journal of Solid State Science and Technology* 8 P357–62
- [32] Ma K Q and Liu J 2007 Nano liquid-metal fluid as ultimate coolant *Physics Letters*, Section A **361** 252–6

- [33] Zhao L, Chu S, Chen X and Chu G 2019 Efficient heat conducting liquid metal/CNT pads with thermal interface materials *Bulletin of Materials Science* **42** 192
- [34] Kong W, Shah N U H, Neumann T v, Vong M H, Kotagama P, Dickey M D, Wang R Y and Rykaczewski K 2020 Oxide-mediated mechanisms of gallium foam generation and stabilization during shear mixing in air *Soft Matter* **16** 5801–5
- [35] Wang X, Fan L, Zhang J, Sun X, Chang H, Yuan B, Guo R, Duan M and Liu J 2019 Printed Conformable Liquid Metal e-Skin-Enabled Spatiotemporally Controlled Bioelectromagnetics for Wireless Multisite Tumor Therapy *Adv Funct Mater* 1907063
- [36] Kanetkar S, Shah N U H, Gandhi R M, Uppal A, Dickey M D, Wang R Y and Rykaczewski K 2023 Fabrication of Multiphase Liquid Metal Composites Containing Gas and Solid Fillers: from Pastes to Foams ACS Applied Engineering Materials
- [37] Shah N U H, Kong W, Casey N, Kanetkar S, Wang R Y-S and Rykaczewski K 2021 Gallium Oxide-Stabilized Oil in Liquid Metal Emulsions *Soft Matter* **17** 8269–75
- [38] Shah N U H, Kanetkar S, Uppal A, Dickey M D, Wang R Y and Rykaczewski K 2022 Mechanism of Oil-in-Liquid Metal Emulsion Formation *Langmuir* **38** 13279–87
- [39] Krisnadi F, Kim S, Im S, Chacko D, Vong M H, Rykaczewski K, Park S and Dickey M D 2024 Printable Liquid Metal Foams That Grow When Watered *Advanced Materials* 2308862
- [40] Gao J, Ye J, Chen S, Gong J, Wang Q and Liu J 2021 Liquid Metal Foaming via Decomposition Agents *ACS Appl Mater Interfaces* **13** 17093–103
- [41] Uppal A, Kong W, Rana A, Wang R Y and Rykaczewski K 2021 Enhancing Thermal Transport in Silicone Composites via Bridging Liquid Metal Fillers with Reactive Metal Co-Fillers and Matrix Viscosity Tuning ACS Appl Mater Interfaces 13 43348–55
- [42] Koh A, Sietins J, Slipher G and Mrozek R 2018 Deformable liquid metal polymer composites with tunable electronic and mechanical properties *J Mater Res* **33** 2443–53
- [43] Pettibone J M, Osborn W A, Rykaczewski K, Talin A A, Bonevich J E, Hudgens J W and Allendorf M D 2013 Surface mediated assembly of small, metastable gold nanoclusters *Nanoscale* **5**
- [44] Rykaczewski K, Anand S, Subramanyam S B S B and Varanasi K K 2013 Mechanism of frost formation on lubricant-impregnated surfaces *Langmuir* **29** 5230–8
- [45] Banhart J 2006 Metal foams: production and stability *Adv Eng Mater* **8** 781–94
- [46] Lyon R N 1952 Liquid Metals Handbook, The Committee on the Basic Properties of Liquid Metals